Revisit of Landau damping and two-stream instabilities at high energy density regime

Jiong-Hang Liang[1], Tian-Xing Hu[1], D. Wu[1,2],* and Zheng-Mao Sheng[1]†

[1] *Institute for Fusion Theory and Simulation, Department of Physics, Zhejiang University, 310058 Hangzhou, China and*

[2] *Collaborative Innovation Center of IFSA, Shanghai Jiao Tong University, Shanghai 200240, China*

(Dated: October 26, 2020)

Classical plasma is typically of low density and/or high temperature, and the basic properties of Landau damping and two-stream instabilities are already well studied. When increasing the plasma density, quantum effect appears and the beam-plasma interactions will show quite different behaviour when compared with classical cases. In this work, the quantum Landau damping and two-steam instabilities are revisited by using quantum hydrodynamic and quantum kinetic theories, with the latter taking into account wave-particle interactions. The similarity and discrepancy of the damping rate of Langmuir Wave between high energy density and classical plasmas are significantly compared and explained. Especially, we found the plasma growth rate behaves as pure two-stream instability without landau damping when countering velocity exceeds a certain threshold, which is different from classical case. Our work might find great applications in inertial confinement fusion researches and also might be of great value in astrophysics studies.

* dwu.phys@zju.edu.cn

† zmsheng@zju.edu.cn

I. INTRODUCTION

High Energy Density Physics (HEDP), especially the warm dense matter (WDM) or hot dense matter (HDM) regime [1–5], has draw much attention in recent years. WDM or HDM widely exists in inertial confinement fusion, and (laboratory) astrophysics studies, with temperatures of $1 \sim 100$ eV and density of $0.1 \sim 10$ solid densities. However, due to the significant high temperatures when compared with condensed matter state and high densities when compared with pure plasma state, experimental and theoretical studies are of great challenges. This is because knowledge of both condensed matter physics and plasma physics needs to be organized together. Therefore many of the foundational properties of WDM or HDM are still open and not well studied.

Among the most fundamental properties of plasmas, Landau damping and two-stream instability are two fundamental properties of plasmas that widely exist in various kinds of physical phenomenon. Landau damping [6] is what defines 'kinetic' efforts which essentially represents wave-particle interaction, while two-stream instability simply represents the excitation of intrinsic oscillation of charged particle in plasma by another group of charged particle flow. In most of cases, two-stream instability can not be treated as a pure fluid instability, since the plasmas in reality always have velocity distributions departing from thermal equilibrium, which means the kinetic effects exist. Although extensively investigated in ideal plasmas [7], under WDM or HDM regime, such properties are seldom studied. In this extreme situation, instabilities behaviour shall differ from classical plasmas in two respects: 1) the equilibrium distribution function becomes Fermi-Dirac function instead of Maxwellian, 2) the quantum mechanical feature, i.e., the wave-like behaviour, of single particle becomes relevant.

The investigation of the properties of dense plasma started from the pioneering works of Bohm and Pines [8, 9] who first utilized the random phase approximation (RPA) approaches to calculate the dynamic response of degenerate plasmas. Under classical plasmas, the RPA approaches reproduce the famous Bohm-Gross wave (BG) with Landau damping, and for degenerate plasmas, one obtains their quantum counterparts. Since then, there are many theoretical attempts to study the influence of quantum effects on two-stream instability. M. Bonitz described the quasi-one-dimensional degenerate plasma in detail and summarized the quantum effects in three-dimensional systems [10–13]; Vladimirov gave an analytical description of collisonless quantum plasma [14]; Manfredi and Haas established the Quantum Hydrodynamics (QHD) theory [15]; Haas gave the fluid expression form of two-stream instability, summarized the differences between various models, and revised QHD under consideration of exchange-correlation effects [16, 17]; M. Akbari-Moghanjoughi compared the difference between fluid approximation and dynamic limit of Wigner-Poisson equation [18–20]; Seunghyeon Son discussed the difference between classical and quantum cases through Lindhard description and given a conclusion that kinetic approach is more accurate than QHD in studying two-stream instability [21].

In this paper, we revisit the Landau damping and two-stream instability by using both QHD and QKT theories. The quantum Landau damping and two-steam instabilities are here revisited by using quantum hydrodynamic and quantum kinetic theories, with the latter taking into account wave-particle interactions. The similarity and discrepancy of the damping rate of Langmuir Wave between high energy density and classical plasmas are significantly compared and explained. Especially, we found the plasma growth rate behaves as pure two-stream instability without landau damping when countering velocity exceeds a certain threshold, which is different from classical case.Especially, we found the plasma growth rate behaves as classical two-stream instability when countering velocity exceeds a certain

threshold.

The article is organized as follows. In Section II, we give a brief introduction to QKT and QHD, and summarize the previous results of two-stream instability under QHD model. In Section III, we take the Lindhard function [22] and give the influence of quantum Landau damping on dispersion relation, and then we study the property of quantum plasma depending on the system density and temperature. In Section IV, we consider the two-stream instability by using QKT theory, and give an explanation for the theoretical difference with QHD model. Finally we compare the effects of quantum dissipative instability under different system parameters. A summary and discussion are given in Section IV.

II. AN INTRODUCTION TO QKT AND QHD

We here give a brief introduction of QKT and QHD. Following the introduction, the existing work on two-stream instabilities based on QHD is also introduced.

A. Quantum Kinetic Theory

Quantum Kinetic Theory (QKT)[23] starts from Wigner function [24]

$$\left(\frac{\partial}{\partial t}+\frac{\mathbf{p}\cdot\nabla_{\mathbf{R}}}{m}\right)f(\mathbf{p},\mathbf{R},t)=\frac{1}{i\hbar}\int\int\frac{d\mathbf{r}d\mathbf{p}'}{(2\pi\hbar)^3}\exp\left(\frac{i(\mathbf{p}-\mathbf{p}')\cdot\mathbf{r}}{\hbar}\right)[U_{eff}(\mathbf{R}+\mathbf{r}/2,t)-U_{eff}(\mathbf{R}-\mathbf{r}/2,t)]f(\mathbf{p}',\mathbf{R},t) \quad (1)$$

where quantum distribution $f(\mathbf{p},\mathbf{R},t)$ is expressed in terms of Schroedinger wave function, $\psi_\alpha(\mathbf{R},t)$, which is characterized by a probability p_α satisfying $\sum_{\alpha=1}^{N}p_\alpha=1$:

$$f(\mathbf{p},\mathbf{R},t)=\sum_{\alpha=1}^{N}\int\frac{d\mathbf{p}}{(2\pi\hbar)^3}\exp\left(\frac{i\mathbf{p}\cdot\mathbf{r}}{\hbar}\right)\times\psi_\alpha^*(\mathbf{R}+\mathbf{r}/2,t)\psi_\alpha(\mathbf{R}-\mathbf{r}/2,t). \quad (2)$$

Here U_{eff} is the potential field, and it is different from the kinetic theory under classical case. When combined with Poisson's equation in integral form

$$U_{eff}(\mathbf{R},t)=U(\mathbf{R},t)+\int d\mathbf{R}'V(\mathbf{R}-\mathbf{R}')\times\int\frac{d\mathbf{p}'}{(2\pi\hbar)^3}f(\mathbf{p}',\mathbf{R},t), \quad (3)$$

one can obtain the linearized longitudinal dielectric function. For electrostatic plasmas, we have

$$\epsilon(\mathbf{k},\omega)=1+u_{\mathbf{k}}\sum_s\chi_s(\mathbf{k},\omega) \quad (4)$$

where $u_{\mathbf{k}}=4\pi e^2/k^2$ is the Fourier component of coulomb interaction of particles with each other, and χ_s is the corresponding density response. According to the work of Bohm and Pines [8, 9], the latter part can be written as

$$\chi_s^c(\omega,\mathbf{k}) = \int \mathrm{d}^3 v \frac{\mathbf{k}\cdot\partial f_s/\partial v}{\omega - \mathbf{k}\cdot\mathbf{v}} \tag{5}$$

and

$$\chi_s^q(\omega,\mathbf{k}) = \int \frac{\mathrm{d}^3 q}{(2\pi)^3} \frac{f_{s,\mathbf{q}-\frac{1}{2}\mathbf{k}} - f_{s,\mathbf{q}+\frac{1}{2}\mathbf{k}}}{\omega - \hbar\mathbf{k}\cdot\mathbf{q}/m} \tag{6}$$

in classical and quantum conditions, respectively. Here one need to note, when comparing the Eqs. (5) and (6), the quantum density response can be reduced to the classical ones by taking the long-wavelength approximations.

The expression of χ_s^q is actually the vacuum polarization bubble resulting from RPA theory. The waves in high damping region can rapidly decay and cannot effectively transport. Therefore, it is appropriate to apply small damping approximation to analyse the property of transport.

At low-temperature limit, where the Fermi distribution reduces to a step function, the real part of density response is

$$\mathrm{Re}\left(\chi_s^q\right) = \frac{mk_\mathrm{F}}{2\pi^2\hbar}\left\{1 - \frac{1}{2\tilde{k}}\left[1-\left(\frac{\tilde{\omega}}{\tilde{k}}-\frac{\tilde{k}}{2}\right)^2\right]\ln\left|\frac{1+\left(\frac{\tilde{\omega}}{\tilde{k}}-\frac{\tilde{k}}{2}\right)}{1-\left(\frac{\tilde{\omega}}{\tilde{k}}-\frac{\tilde{k}}{2}\right)}\right| + \frac{1}{2\tilde{k}}\left[1-\left(\frac{\tilde{\omega}}{\tilde{k}}+\frac{\tilde{k}}{2}\right)^2\right]\ln\left|\frac{1+\left(\frac{\tilde{\omega}}{\tilde{k}}+\frac{\tilde{k}}{2}\right)}{1-\left(\frac{\tilde{\omega}}{\tilde{k}}+\frac{\tilde{k}}{2}\right)}\right|\right\} \tag{7}$$

and the imaginary part is

$$\mathrm{Im}\left(\chi_s^q\right) = \begin{cases} -\dfrac{mk_\mathrm{F}}{\hbar^2}\dfrac{1}{4\pi\tilde{k}}2\tilde{\omega}, & \text{with } (\tilde{\omega}/\tilde{k}+\tilde{k}/2) < 1 \\ -\dfrac{mk_\mathrm{F}}{\hbar^2}\dfrac{1}{4\pi\tilde{k}}\left[1+\left(\dfrac{\tilde{\omega}}{\tilde{k}}-\dfrac{\tilde{k}}{2}\right)^2\right], & \text{with } \left|\tilde{\omega}/\tilde{k}-\tilde{k}/2\right| < 1 < (\tilde{\omega}/\tilde{k}+\tilde{k}/2) \\ 0, & \text{with } \left|\tilde{\omega}/\tilde{k}-\tilde{k}/2\right| > 1 \end{cases}$$

Here $\tilde{\omega} = \omega/(\hbar k_\mathrm{F}^2/m)$ is the normalized frequency, and $\tilde{k} = k/k_\mathrm{F}$ is the normalized wave vector. This result is derived by Lindhard [22] under small damping approximation. Considering the limit of $\tilde{\omega} \gg \tilde{k}$, which is the same way to analyse the electron Langmuir waves in classical plasmas, we get the dispersion relation

$$\omega_\mathrm{LW}(k) = \left(\omega_\mathrm{p}^2 + \langle v^2\rangle k^2 + \frac{\hbar^2 k^4}{4m_\mathrm{e}^2}\right)^{1/2} \tag{8}$$

which is derived by Klimontovich and Silin [25]. For zero temperature fermions, we have

$$\langle v^2\rangle = \frac{3}{5}\left(\frac{p_\mathrm{F}}{m}\right)^2 \tag{9}$$

where $p_\mathrm{F} = \hbar k_\mathrm{F} = \hbar(3\pi^2 n)^{1/3}$ is the Fermi momentum.

B. Quantum Hydrodynamics

Haas and Manfredi [15] derived the Quantum Hydrodynamics equations from the Wigner-Poisson equantions

$$\frac{\partial n}{\partial t} + \nabla \cdot (n\mathbf{u}) = 0 \tag{10}$$

$$\frac{\partial \mathbf{u}}{\partial t} + \mathbf{u} \cdot \nabla \mathbf{u} = \frac{e}{m}\nabla\Phi - \frac{1}{mn}\nabla\mathbf{P} \tag{11}$$

where the density, velocity and pressure are respectively given by

$$n = \int \frac{d\mathbf{p}}{(2\pi\hbar)^3} f(\mathbf{p}, \mathbf{R}, t) \tag{12}$$

$$\mathbf{u} = \frac{1}{nm} \int \frac{d\mathbf{p}}{(2\pi\hbar)^3} \mathbf{p} f(\mathbf{p}, \mathbf{R}, t) \tag{13}$$

$$\mathbf{P} = m \int \frac{d\mathbf{p}}{(2\pi\hbar)^3} (\mathbf{v}^2 - \mathbf{u}^2) f(\mathbf{p}, \mathbf{R}, t) \tag{14}$$

The pressure can be separated into classical part and quantum part. The quantum part can be written as

$$\mathbf{P}^{\mathrm{Q}} = -\frac{\hbar^2}{2m} \frac{\nabla^2\sqrt{n}}{\sqrt{n}} \tag{15}$$

whose gradient, $-\nabla\mathbf{P}^{\mathrm{Q}}$, is also called Madelung term [26] or Bohm Potential [8, 9].

Linearizing the above formula, we can also get the dispersion relation of Langmuir wave, Eqs. (8), which means that QHD and QKT are mutually unified in the case of long-wavelength approach.

C. Two-stream Instability Analysis via QHD

Two-stream instability is a basic and crucial research content in classical plasma. In the study of collective effects at quantum regime such as fast ignition and white dwarfs, two-stream instabilities also significantly influence the transport of charged particles in plasmas.

When ignoring the kinetic effect and adopting the QHD approach [16], we have

$$1 - \frac{\omega_{\mathrm{pe}}^2}{(\omega + \mathbf{k}\cdot\mathbf{u}_0)^2 - \omega_{\mathrm{u}}^2} - \frac{\omega_{\mathrm{be}}^2}{(\omega - \mathbf{k}\cdot\mathbf{u}_0)^2 - \omega_{\mathrm{u}}^2} = 0 \tag{16}$$

where $\omega_{\rm pe} = \omega_{\rm be} = \omega_{\rm p}$ for two-stream case. The different considerations lead to different values of $\omega_{\rm u}$: 1) Classical zero temperature case, $\omega_{\rm u}^2 = 0$; 2) Classical Fermi distribution case, $\omega_{\rm u}^2 = \langle v^2 \rangle k^2$ with $\langle v^2 \rangle = (3/5)v_{\rm F}^2$; and 3) Quantum condition, $\omega_{\rm u}^2 = \langle v^2 \rangle k^2 + \hbar^2 k^4 / 4m_{\rm e}^2$. As expected, the expression of dispersion relation is also naturally consistent with the QKT Langmuir wave under the long-wavelength approximation. Now we can expand the expression into polynomial form $(\omega^2 + k^2 u_0^2 - \omega_{\rm u}^2)^2 - 4k^2 u_0^2 \omega^2 - 2(\omega^2 + k^2 u_0^2 - \omega_{\rm u}^2)\omega_p^2 = 0$. Then we obtain the solution of dispersion relation

$$\omega^2 = \omega_{\rm p}^2 + \omega_{\rm u}^2 + k^2 u_0^2 \pm [\omega_{\rm p}^4 + 4k^2 u_0^2 (\omega_{\rm p}^2 + \omega_{\rm u}^2)]^{1/2}. \tag{17}$$

The solution has two branches, one is a stable solution with $\omega^2 > 0$, and the other is an unstable solution with $\omega^2 < 0$, which represents the region that leads to the two-stream instability. The unstable solution satisfies

$$(k^2 u_0^2 - \omega_{\rm u}^2)(2\omega_{\rm p}^2 + \omega_{\rm u}^2 - k^2 u_0^2) < 0 \tag{18}$$

1) For classical zero temperature case, $\omega_{\rm u}^2 = 0$, instability region always exists. The interval of instability region is $k < \sqrt{2}\omega_{\rm p}/u_0$.

2) For classical Fermi distribution case, we have $\omega_u^2 = \langle v^2 \rangle k^2$. In this case, there is a certain threshold for the appearance of the instability region: $u_0^2 > \langle v^2 \rangle$, which means two-stream instability begins to emerge when the countering drift velocity is greater than the respective thermal velocity [27, 28]. The instability region satisfies $k < \sqrt{2}\omega_{\rm p}/(u_0^2 - \langle v^2 \rangle)^{1/2}$.

3) For quantum condition, we have $\omega_{\rm u}^2 = \langle v^2 \rangle k^2 + \hbar^2 k^4 / 4m_{\rm e}^2$. The threshold that instability region begins to emerge is the same as in the second case, $u_0^2 > \langle v^2 \rangle$. When $\langle v^2 \rangle < u_0^2 < \langle v^2 \rangle + \sqrt{2}\hbar\omega_{\rm p}/m$, the instability region satisfies $k < 2mU^{1/2}/\hbar$ where $U = u_0^2 - \langle v^2 \rangle$. When $u_0^2 > \langle v^2 \rangle + \sqrt{2}\hbar\omega_{\rm p}/m$, a new stable region $[k_a, k_b]$ begins to appear:

$$k_a^2 = (2m^2/\hbar^2)[U - (U^2 - 2\hbar^2\omega_{\rm p}^2/m^2)^{1/2}] \tag{19}$$

and

$$k_b^2 = (2m^2/\hbar^2)[U + (U^2 - 2\hbar^2\omega_{\rm p}^2/m^2)^{1/2}] \tag{20}$$

For Fermi distribution at zero temperature, $U = v_0^2 - 3/5 v_{\rm F}^2$.

From Fig. 1, we can intuitively understand that the influence of temperature or Fermi distribution will increase the area of two-stream instability, while the maximum growth rate will decrease. Comparing the second and third case, we find that quantum correction will further expand the instability interval and simultaneously form a new stable region in it, thereby splitting it into two growth intervals.

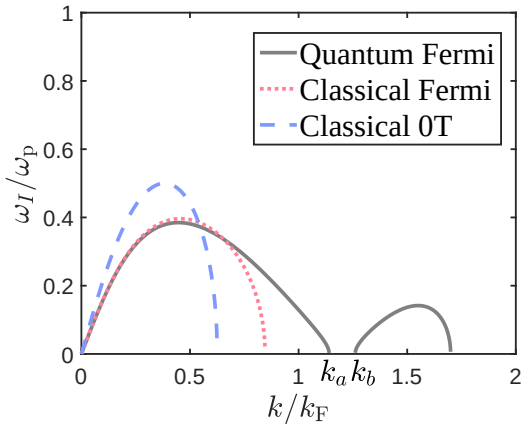

FIG. 1. Growth rates of different conditions at countering drift $u_0 = 1.15v_F$, with parameters: $T_e = 0$, and $n_p = n_b = 10^{24}\text{cm}^{-3}$.

III. REVISITING LANDAU DAMPING

In this section, we compare the quantum Landau damping with both QKT and QHD theories. QHD is a fluid theory which ignoring the wave-particle interactions. In comparison, QKT is relatively a more complete theory, although the analytical solution of QKT is not easy to follow.

According to Eqs. (8), when compared with the dispersion relation of classical Langmiur waves, $\omega(k) = (\omega_p^2 + \langle v_{th}^2\rangle k^2)^{1/2}$, the Fermi distribution, physically corresponding to the Pauli principle, promotes particles to fill the lowest energy levels and provides the system a minimum average kinetic energy. For this reason, there is no absolute "cold" plasma at low-temperature limits. There is another wave structure called electron acoustic wave (EAW) which is certainly nonlinear and strongly damped, but can still exist in a plasma. It was previously described by Hollway and Dorning [29] in classical plasma, and they gave the acoustic-form dispersion relation, $\omega = 1.31kv_{th}$ for small k, which is related to thermal pressure. Therefore, EAWs will not disappear at low-temperature conditions, which is an important difference from the classical plasmas.

Let us consider the limit that $\tilde{k}$ ($\tilde{k} > 0$) approach zero and $\tilde{\omega}/\tilde{k}$ has a finite value. According to the approximation $\ln\left|1 - (\frac{\tilde{\omega}}{\tilde{k}} \pm \frac{\tilde{k}}{2})\right| \approx \ln\left|1 - \frac{\tilde{\omega}}{\tilde{k}}\right| \pm \frac{\tilde{k}}{2\left|1-\frac{\tilde{\omega}}{\tilde{k}}\right|} + O(\tilde{k}^2)$, we can expand the real part of quantum dielectric function, and the $\tilde{\omega}/\tilde{k}$ relation of quantum electron acoustic waves satisfies

$$-\frac{\tilde{\omega}}{\tilde{k}}\ln\left|\frac{1+\frac{\tilde{\omega}}{\tilde{k}}}{1-\frac{\tilde{\omega}}{\tilde{k}}}\right| + 2 = 0 \tag{21}$$

Then we have the linearized dispersion relation of EAWs at quantum condition, $\omega_{EAW} \approx 0.834kv_F$.

Using Eqs. (7) and (8), we can get the real solution of dispersion relation and obtain the damping rates by small damping approximation,

$$\gamma = -\epsilon_I(k, \omega_R)/\left(\partial\epsilon_R/\partial\omega\right)_{\omega_R}. \tag{22}$$

As shown in Fig. 2, the resonance curve $\omega^+(k)$ cut the $\omega - k$ plane into undamping region and damping region. For the waves whose phase velocity is greater than Fermi velocity, there are no particles satisfied the velocity condition

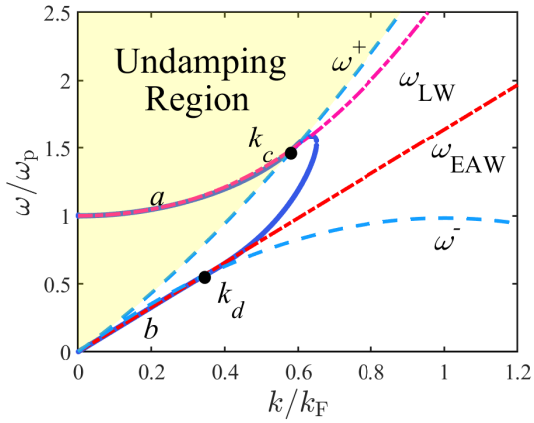

FIG. 2. Real dispersion relation of longitudinal oscillations of a degenerate electron gas by QKT with $T_{\rm e} = 0$, and $n_{\rm e} = 10^{24}{\rm cm}^{-3}$. Here a is the optical mode and b is the acoustic mode. k_c and k_d respectively represent damping turning points of two modes. $\omega^{\pm} = \hbar k/2m(2k_F \pm k)$ is the kinetic resonance frequency for particles on Fermi sphere.

and hence no particle can resonance with waves and contribute to Landau damping. The intersection of optical mode and resonance curve $\omega^+(k)$ indicates a turning point k_c which shows Landau damping occurs for the part $k > k_c$ of optical mode. Another turning point k_d exists at the intersection of acoustic mode and resonance curve $\omega^-(k)$. However, unlike optical mode, the acoustic mode is always damped.

Let us consider the influence of electron density on dispersion relation of the degenerate system. As shown in the Fig. 3, it is obvious that the optical mode approaches to the classical electron Langmuir waves as density decreases. Another important point is that the acoustic mode approaches the k-axis simultaneously and deviates from the kinetic resonance frequency (ω^-), which is consistence with the classical condition at low density limit.

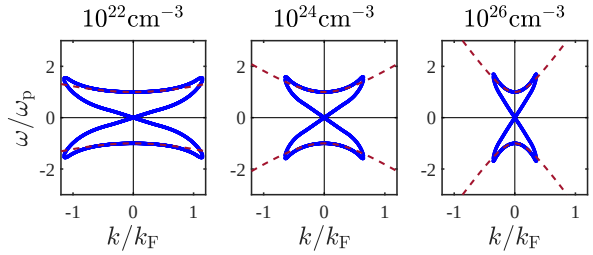

FIG. 3. The real part of longitudinal dispersion relation as the density changes shown by the solid lines (blue). The dashed lines represent the theoretical approach of optical mode, $\omega_{\rm LW}(k)$ (red).

The dissipative undamping region limit $k_{\rm c}$ of optical mode is a parameter which shows the difference between quantum condition and classical condition. The formation of undamping region is due to the steep edge of Fermi-Dirac distribution, which is different from the undamping region based on Debye Shielding at classical condition. The normalized kinetic resonance frequency is

$$\frac{\omega^{\pm}}{\omega_{\rm p}} = \frac{\hbar k_{\rm F}^2}{2m\omega_{\rm p}}\left(2\frac{k}{k_{\rm F}} \pm \frac{k^2}{k_{\rm F}^2}\right) = \frac{\epsilon_{\rm F}}{\hbar\omega_{\rm p}}\left(2\frac{k}{k_{\rm F}} \pm \frac{k^2}{k_{\rm F}^2}\right) \tag{23}$$

According to Eqs.(8) and (23), the undamping limit $k_{\rm c}$ satisfies

$$\frac{k_c^3}{k_F^3}+\frac{2}{5}\frac{k_c^2}{k_F^2}-\frac{\hbar^2\omega_{pe}^2}{\epsilon_F^2}=0 \tag{24}$$

As shown in Fig.4(b), the first order slope of resonance curve $\epsilon_F/\hbar\omega_p$ increases with density, which means the area of undamping region in $\omega-k$ plane decreases simultaneously. The tendency of curve $k_c(n)$ also represents the same conclusion. It should be noted that the absolute value of k_c increases with density in the contrary, because the Fermi wave vector k_F is proportional to $n^{1/3}$, shown by the solid line in Fig. 4(a).

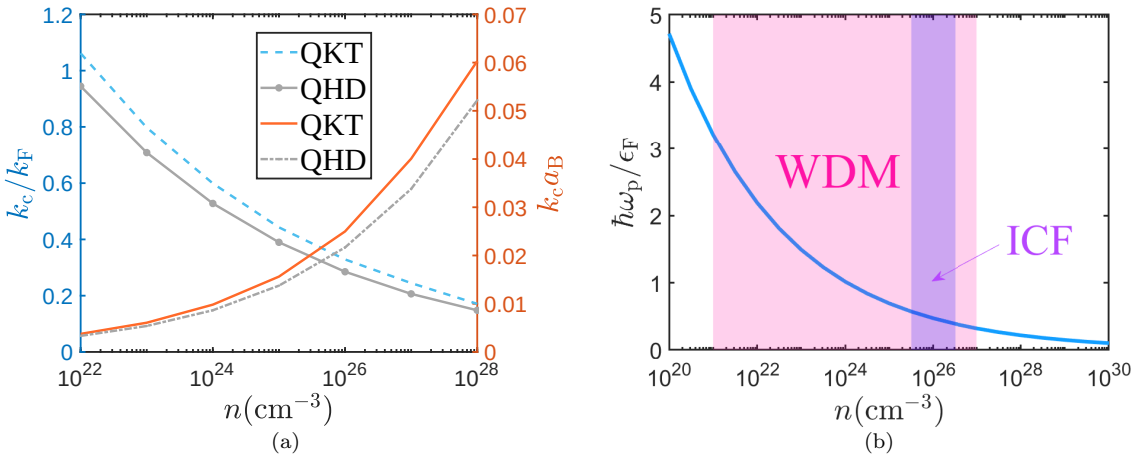

FIG. 4. (a) Various values of quantum undamping region limit k_c of optical mode with $T_e=0$ as the density changes using QKT and QHD. Here, $a_B=52.9$pm is the hydrogen Bohr radius. (b) The ratio of plasmon energy and Fermi energy of degenerate system decreases as the density increases.

The low-temperature limit theory has pointed out some difference between classical and quantum condition, however, cannot obtain an accurate result at finite temperature. Hence we can directly solve Eqs. (6) by using small damping approximation from the beginning. The real part of dispersion relation can only be given analytically at some limit cases [30, 31]. And the imaginary part can be found by theoretical approach

$$\mathrm{Im}\left(\chi_s^q(\omega,k)\right)=\frac{2e^2m^2}{\beta k^3\hbar^4}\ln\left(\frac{\tilde{f}_-(\omega,k)}{\tilde{f}_+(\omega,k)}\right) \tag{25}$$

where

$$\tilde{f}_\pm(\omega,k)=1+\exp\left[\mu\beta-\left(\frac{\omega}{k}\pm\frac{k}{2}\right)^2\frac{\beta}{2m}\right] \tag{26}$$

Hence we can use Eqs. (22) and the real part solutions to get the damping rates.

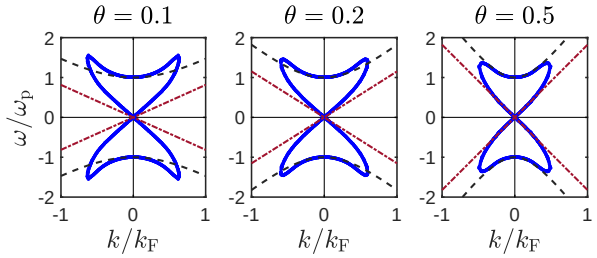

FIG. 5. The solid lines (blue) represent the real part of dispersion relation as the temperature $\theta = k_{\rm B}T/\epsilon_{\rm F}$ changes. The dashed line (grey) is classical Langmuir waves $\omega = (\omega_{\rm p}^2 + \langle v_{\rm th}^2\rangle k^2)^{1/2}$. The dotted line (red) is classical EAWs, $\omega = 1.31 k v_{\rm th}$ [29].

We plot the real part of dispersion relation in Fig. 5. High temperature breaks the steep edge of Fermi distribution to be smooth and narrow the difference between quantum theory and classical limit. For this reason, the undamping region will disappear. However, at relatively low temperature, there is very few particles with large momentum which can resonance with waves. Hence, just like what we have implemented at low-temperature limit case, here we have $2/(e^{\beta(\hbar^2 k_{\rm t}^2/2m-\mu)}+1) > 1/n$ where the factor 2 stands for spin of electron. Then we get $k_{\rm t}^2 = 2m/\hbar^2[\mu + \frac{1}{\beta}\ln(2n)]$.

Replacing $k_{\rm F}$ at quantum low temperature with $k_{\rm t}$, and simultaneously considering the energy conservation, we have the approximate resonance frequency for particles at finite temperature:

$$\omega_{\pm} = k\sqrt{\frac{2}{m}\left(\mu + \frac{1}{\beta}\ln(2n)\right)} \pm \frac{\hbar k^2}{2m} \tag{27}$$

Then we can determine the undamping region limit k_c according to the intersection of resonance frequency curve and Langmuir wave curve Eqs.(8), shown by the dashed line in the FIG.6.

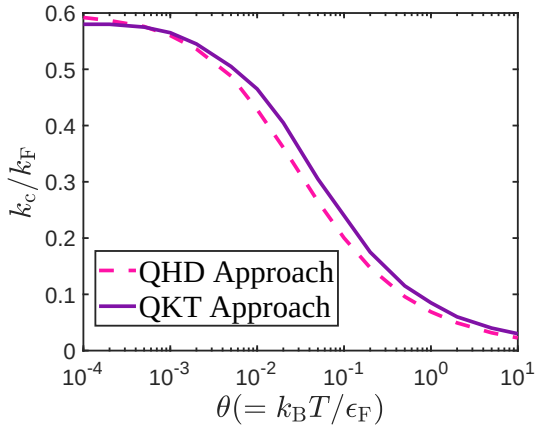

FIG. 6. The undamping region limit of optical mode ($n = 10^{24}{\rm cm}^{-3}$) at finite temperature according to the approximate resonance condition is shown by the dashed line. The solid line represents the theoretical approach of imaginary part of dielectric function.

The tendency of two curves in Fig. 6 is basically the same. Therefore, the reason for the formation of dissipative undamping region is indeed the particularity of Fermi distribution. As shown in the figure, the value of $k_{\rm c}/k_{\rm F}$ tends to zero as temperature increases. It means at high temperature limit, since the Fermi distribution is equivalent to the

Maxwellian, the undamping region disappears, which is consistent with the classical situation.

IV. REVISIT OF TWO-STREAM INSTABILITY

In this section, we compare the two-stream instability results of QKT and QHD studies. Here, in order to maintain symmetry and facilitate research, we study non-relativistic countering-stream case, which can also be obtained from two-stream case by coordinate transformation.

$$\epsilon(\mathbf{k},\omega) = 1 + u_{\mathbf{k}}\chi_{pe}\left(\mathbf{k},\omega+\mathbf{k}\cdot\mathbf{u_0}\right) + u_{\mathbf{k}}\chi_{be}\left(\mathbf{k},\omega-\mathbf{k}\cdot\mathbf{u_0}\right) \tag{28}$$

where χ_{pe} and χ_{be} respectively represent the density response of background plasma and plasma beam.

Now we can add the previously omitted kinetic Landau damping to the theoretical results of QHD. Due to the existence of two parts of countering electrons, their respective undamping regions will overlap. When the countering speed exceeds a certain threshold, the overlapping part will form a new exact dissipative undamping region.

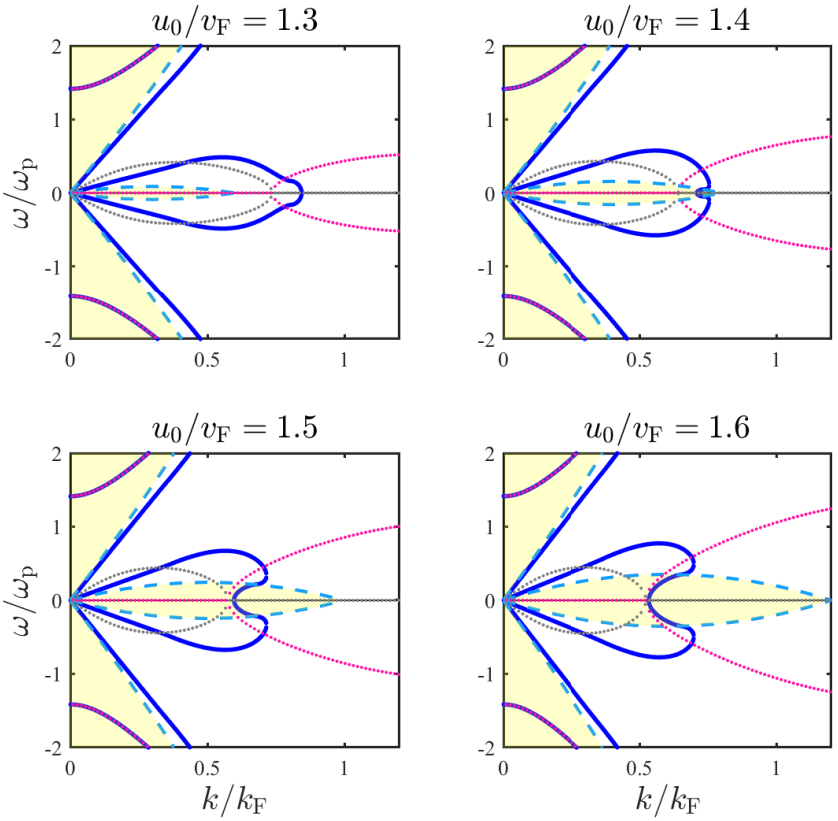

FIG. 7. The same as Figure 2, but for countering-stream case ($T_\mathrm{e} = 0, n_\mathrm{p} = n_\mathrm{b} = 10^{24}\mathrm{cm}^{-3}$). Solid lines (blue) represent the numerical solution of QKT, and dotted lines represent the real (red) and imaginary (grey) solution of QHD. The enclosed dashed curves (light blue) form a new dissipative undamping region.

In Fig.7, the increase in countering velocity causes the new undamping region to expand, so as to completely cover

the first growth interval of two-stream instability. According to the intersection of two kinetic resonance frequency curves, we have the vertex of new dissipative undamping region:

$$k = 2\left(mu_0/\hbar - k_{\mathrm{F}}\right) \tag{29}$$

And this stable region also coincides with part or all of two-stream instability growth region. Combing the Eqs.(19) and (29), we can get the countering velocity required when the dissipative undamping region and growth region is completely covered

$$\frac{u_{\mathrm{c}}^2}{v_{\mathrm{F}}^2} + \frac{13}{5} - 4\frac{u_{\mathrm{c}}}{v_{\mathrm{F}}} + \sqrt{(\frac{u_{\mathrm{c}}^2}{v_{\mathrm{F}}^2} - \frac{3}{5})^2 - \frac{1}{2}\frac{\hbar^2\omega_{\mathrm{p}}^2}{\epsilon_{\mathrm{F}}^2}} = 0 \tag{30}$$

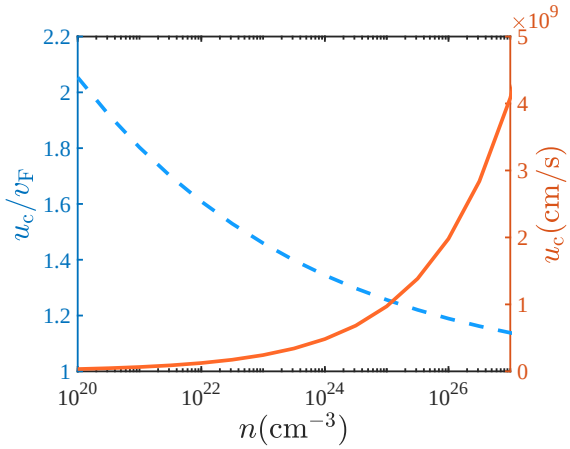

FIG. 8. the value of countering velocity threshold with the change of electron density.

According to Equ.(30), we plot the tendency of velocity threshold with electron density in Fig.8. As density increases, the ratio of threshold velocity to Fermi velocity decreases, while the absolute value increases, which is consistent with the change trend of k_{c} in Section II.

When the countering velocity is greater than the threshold, the instability of this region appears as pure two-stream growth rate without the influence of Landau damping. From the perspective of distribution function, when phase velocity of waves is located at the 'gap' between two parts of electron distribution, waves can be directly excited by two-stream growth rate without Landau damping.

As the countering velocity increases, the results of QHD and QKT gradually conincide. When the stable mode just appeared in QKT ($u_0 \approx u_{\mathrm{c}}$), the difference between two theories are relatively large, mainly because the approximation of QHD has a certain error in short-wavelength region.

Quantum correction is the reason for the formation of this new dissipative stable region. Considering the dispersion relation of Fermi system in classical case, we find that the similar stable region is an open interval composed of two rays, which is different from the closed interval in quantum case. Thus, when $u_0/v_{\mathrm{F}} > 1$, the entire range of two-stream instability is completely within this region in classical case.

Therefore, in quantum case, within a certain countering velocity range, wave growth rate is the result of combined

effect of two-stream instability and wave-particle resonance, which cannot be considered separately.

In Section II, we mentioned that the increase in temperature will lead to the reduction of undamping region, which is consistent with classical case at high temperature limit. Therefore, temperature is one of factors that affect two-stream instability. According to Equ.(27) and Equ.(19), we can get the vertex of undamping region

$$k = \frac{2m}{\hbar}\left(u_0 - \sqrt{\frac{2}{m}\left(\mu + \frac{1}{\beta}\ln(2n)\right)}\right) = \frac{2m}{\hbar}\left(u_0 - v_\mu\right) \tag{31}$$

Similarly, we can get the countering velocity threshold where dissipative undamping coincides with the first growth region of two-stream instability

$$u_{\rm c}^2 - 4v_\mu u_{\rm c} + 2v_\mu^2 + \langle v^2\rangle + \sqrt{(u_{\rm c}^2 - \langle v^2\rangle)^2 - \frac{2\hbar^2\omega_{\rm p}^2}{m^2}} = 0 \tag{32}$$

We plot the solution of Equ.(32) in Fig.9, we can see that as temperature increases, the equivalent thermal velocity is also increasing, which means that a higher velocity is required to cause the appearance of two-stream instability. And the threshold velocity rises faster, which means that the higher system temperature, the higher countering velocity is needed to make two-stream instability completely free of Landau damping. However, a high countering velocity will cause two-stream instability to be insignificant, and simultaneously the theory of relativity needs to be considered, which also requires the basic model to be revised. Therefore, in high temperautre region, two-stream instability is bound to be accompanied by a certain Landau damping.

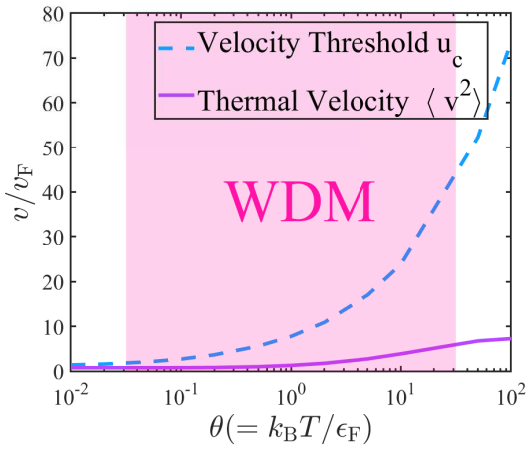

FIG. 9. the value of countering velocity threshold with the change of temperature ($n = 10^{24}\mathrm{cm}^{-3}$).

V. CONCLUSION

In this paper, we discussed the quantum effect of two-stream instability in high density plasmas by means of quantum kinetic theory and quantum hydrodynamics. The discrepancies of these two theoretical framework are

caused by wave-particle interaction, i.e., kinetic effects, which is ignored by QHD. We conclude that, firstly, the Fermi statistic effect yields a stable region without Landau damping, which is further deformed by single-particle quantum effect, namely, the Bohm potential. This stable region shrinks as the temperature rises, which means the quantum effect being concealed by thermal effect. And secondly, the unstable region of two-stream instability is split into two parts by Bohm effect, and one of which is located at the dissipative undamping region thus yielding a pure two-stream instability growth region. Last but not least, there exists a threshold drift velocity beyond which the two-stream instability decouples with Landau damping and become a pure fluid instability. This threshold also increases as temperature rises.

ACKNOWLEDGMENTS

This work was supported by the National Natural Science Foundation of China (Grant No. 11875235, 12075204), Strategic Priority Research Program of Chinese Academy of Sciences (Grant No. XDA250050500) and Science Challenge Project (No. TZ2016005).

[1] T. G. White, N. J. Hartley, B. Borm, B. J. B. Crowley, J. W. O. Harris, D. C. Hochhaus, T. Kaempfer, K. Li, P. Neumayer, and L. K. and Pattison. Electron-ion equilibration in ultrafast heated graphite. *Physical Review Letters*, 112(14):145005, 2014.

[2] A. Pelka, G. Gregori, D. O. Gericke, J. Vorberger, S. H. Glenzer, M. M. Gnther, K. Harres, R. Heathcote, A. L. Kritcher, and N. L. and Kugland. Ultrafast melting of carbon induced by intense proton beams. *Physical Review Letters*, 105(26):265701, 2010.

[3] G. M. Dyer, A. C. Bernstein, B. I. Cho, J. Osterholz, and T. Ditmire. Equation-of-state measurement of dense plasmas heated with fast protons. *Physical Review Letters*, 101(1):015002, 2008.

[4] J. Lindi. Development of the indirect-drive approach to inertial confinement fusion and the target physics basis for ignition and gain. *Physics of Plasmas*, 2(11):3933–4024.

[5] X. T. He, J. W. Li, Z. F. Fan, L. F. Wang, J. Liu, K. Lan, J. F. Wu, and W. H. Ye. A hybrid-drive nonisobaric-ignition scheme for inertial confinement fusion. *Physics of Plasmas*, 23(8):082706, 2016.

[6] L. D. Landau. On the vibrations of the electronic plasma. *Zhurnal Eksperimentalnoi I Teoreticheskoi Fiziki*, 16(7):574–586, 1946.

[7] F. F. Chen. *Introduction to plasma physics and controlled fusion.*, volume 1. Springer, 1984.

[8] D. Pines and D. Bohm. A collective description of electron interactions: II. Collective vs individual particle aspects of the interactions. *Physical Review*, 85(2):338–353, 1952.

[9] D. Bohm and D. Pines. A collective description of electron interactions: Iii. coulomb interactions in a degenerate electron gas. *Physical Review*, 92(3):609–625, 1953.

[10] M. Bonitz, T. Dornheim, Zh. A. Moldabekov, S. Zhang, P. Hamann, A. Filinov, K. Ramakrishna, and J. Vorberger. Ab initio simulation of warm dense matter. *Physics of Plamsas*, 27(4), 2020.

[11] M. Bonitz, Zh. A. Moldabekov, and T. S. Ramazanov. Quantum hydrodynamics for plasmas–Quo vadis ? *Physics of Plasmas*, 26(9), 2019.

[12] M. Bonitz, R. Binder, D. C. Scott, S. W. Koch, and D. Kremp. Theory of plasmons in quasi-one-dimensional degenerate plasmas. *Physical Review E*, 49(6):5535–5545, 1994.

[13] M. Bonitz. *Quantum Kinetic Theory*. Springer International Publishing, 2016.

[14] S.V. Vladimirov and Yu O. Tyshetskiy. On description of a collisionless quantum plasma. *Physics-uspekhi*, 54(12):1243–1256, 2011.

[15] G. Manfredi and F. Haas. Self-consistent fluid model for a quantum electron gas. *Physical Review B*, 64(7):075316, 2001.

[16] F. Haas. *Quantum Plasmas*. Springer-Verlag New York, 2011.

[17] F. Haas. Kinetic theory derivation of exchange-correlation in quantum plasma hydrodynamics. *Plasma Physics and Controlled Fusion*, 61(4):044001.

[18] M. Akbari-Moghanjoughi, M. Mohammadnejad, and A. Esfandyari-Kalejahi. Electrostatic two-stream instability in fermi-dirac plasmas. *Astrophysics and Space Science*, 361(9):307, 2016.

[19] M. Akbarimoghanjoughi. Hydrodynamic limit of wigner-poisson kinetic theory: Revisited. *Physics of Plasmas*, 22(2):022103, 2015.

[20] M. Mohammadnejad and M. Akbari-Moghanjoughi. Two stream ion acoustic wave instability in warm dense plasmas. *Astrophysics and Space Science*, 364(2):23, 2019.

[21] S. Son. Two stream instabilities in degenerate quantum plasmas. *Physics Letters A*, 378(34):2505–2508, 2014.

[22] J. Lindhard. On the properties of a gas of charged particles. *Matematisk-fysiske Meddelelser Kongelige Danske Videnskabernes Selskab*, 28(8):1–57, 1954.

[23] L.P. Kadanoff and G. Baym. *Quantum Statistical Mechanics*. W.A. Benjamin, Inc. New York, 1962.

[24] E. P. Wigner. On the quantum correction for thermodynamic equilibrium. *Physical Review*, 40(5):749–759, 1932.

[25] Y.L. Klimontovich and V.P. Silin. *o spektrakh sistem vzaimodeistvuyushchikh chastits. 23(2):151–160, 1952.

[26] E. Madelung. Quantentheorie in hydrodynamischer form. *Ztschrift fr Physik*, 40(3-4):322–326, 1927.

[27] T.M. O'Neil and J.H. Malmberg. Transition of the dispersion roots from beam-type to landau-type solutions. *Physics of Fluids*, 11(8):1754–1760, 1968.

[28] G. Francis, A. K. Ram, and A. Bers. Finite temperature effects on the space-time evolution of two-stream instabilities. *Physics of Fluids*, 29(1):255–261, 1986.

[29] J.P. Holloway and J. J. Dorning. Undamped plasma waves. *Physical Review A*, 44(6):3856–3868, 1991.

[30] I. I. Goldman. Oscillations of a degenerate electron fermi gas. *Zhurnal Eksperimentalnoi I Teoreticheskoi Fiziki*, 17(8):681–685, 1947.

[31] V.P. Silin. *k teorii spektra vozbuzhdenii sistemy mnogikh chastits. *Zhurnal Eksperimentalnoi I Teoreticheskoi Fiziki*, 23(6):641–648, 1952.